Oxidation of GaSb(100) and its control studied by scanning tunneling microscopy and spectroscopy

J. Mäkelä,[1,a)] M. Tuominen,[1] M. Yasir,[1] M. Kuzmin,[1,2] J. Dahl,[1] M. P. J. Punkkinen,[1] P. Laukkanen,[1,a)] K. Kokko,[1] and R. M. Wallace[3,a)]
[1]*Department of Physics and Astronomy, University of Turku, FI-20014 Turku, Finland*
[2]*Ioffe Physical-Technical Institute, Russian Academy of Sciences, St. Petersburg 194021, Russian Federation*
[3]*Department of Materials Science and Engineering, The University of Texas at Dallas, Richardson, Texas 75080, USA*

(Received 22 May 2015; accepted 2 August 2015; published online 12 August 2015)

Atomic-scale knowledge and control of oxidation of GaSb(100), which is a potential interface for energy-efficient transistors, are still incomplete, largely due to an amorphous structure of GaSb(100) oxides. We elucidate these issues with scanning-tunneling microscopy and spectroscopy. The unveiled oxidation-induced building blocks cause defect states above Fermi level around the conduction-band edge. By interconnecting the results to previous photoemission findings, we suggest that the oxidation starts with substituting second-layer Sb sites by oxygen. Adding small amount of indium on GaSb(100), resulting in a (4×2)-In reconstruction, before oxidation produces a previously unreported, crystalline oxidized layer of (1×3)-O free of gap states. © *2015 AIP Publishing LLC*.
[http://dx.doi.org/10.1063/1.4928544]

As traditional silicon-based electronics components are approaching their fundamental limits in scalability; more and more attention has been paid to the research and development of other materials, potential to be incorporated in the established Si platform. The III–V semiconductors (e.g., GaAs, GaSb, GaInAs, InP), which are already used widely in optoelectronics and fast RF-transistor circuits, form one of the most mature material systems to be integrated with the Si-based electronics, in order to develop high-performance devices. For instance, improved carrier mobility characteristics could be achieved with III–V semiconductors. However, one major problem with III–V's has been poor quality of oxide/III–V interfaces. The interface between a semiconductor and a high-permittivity (high-κ) dielectric layer is the heart of the metal-oxide-semiconductor (MOS) transistors, for example. To work properly, the interface must be stable, contain a low enough density of electronic defect states around the band gap, and form a high enough barrier for electric carriers. The SiO_2/Si meets strict technological requirements, but insulator/III–V interfaces still contain too many defect states for MOS applications. The main source of defects is known to be the oxidation of III–V surfaces that is a very exothermic reaction and hardly avoidable during the insulator/III–V growth. Thus, it is relevant to understand and control the effects of the III–V oxidation to reduce the interface defect densities (D_{it}) to a comparable level, as it is in today's SiO_2/Si interfaces.[1–3] Note that SiO_2/Si interfaces have a D_{it} of $\sim 10^{13}/cm^2$ eV as grown. Only after subsequent passivation by hydrogen, this is reduced to the mid-10^{10} range. Thus, the key challenge in III–V's may really be a suitable oxide that permits interface passivation by an appropriate passivating agent. For III–V's oxide-interfaces, the lowest reported D_{it} values are in $10^{11}/cm^2$ eV to $10^{12}/cm^2$ eV range.[2]

Gallium antimonide (GaSb) has attracted an increasing interest as for the channel material of future MOS transistors, in particular, due to a superior mobility of holes in GaSb.[4–17] The GaSb oxidation at the insulator interfaces such as atomic-layer-deposited (ALD) Al_2O_3/GaSb and HfO_2/GaSb has been found to cause various oxidation states of GaSb including Ga_2O, Ga_2O_3, Sb_2O_3, and/or Sb_2O_5 according to x-ray photoelectron spectroscopy (XPS) measurements.[10,18] By obtaining interrelationship between the interfacial chemistry from, for example, XPS measurements and capacitance-voltage (C-V) characterization of the same interfaces, the effects of the oxidation states on the electrical properties of the interfaces have been clarified: it is interesting that neither Ga_2O_3- nor Sb_2O_3-type interface phase is necessarily harmful to the electrical performance.[4,10,14] In contrast, the decomposition of Sb_2O_3 into lower Sb oxidation-state phases and/or elemental Sb during the growth and/or post-growth heating of the interface has been observed to cause defect states in the GaSb band-gap area.[4,10,14] Furthermore, computational results have shown that oxygen-rich HfO_2/GaSb interfaces are free of band-gap defect states,[12] and that the oxidation starts with O incorporation into the middle of Sb-Ga dimer so that no band-gap state is introduced.[13] To recapitulate, the previous results indicate that a properly tailored oxidation of GaSb does not cause the defect states in the band gap. Indeed, this is a promising result because, in practice, it is very difficult (or impossible) to avoid the oxygen interaction with a semiconductor surface during the oxide or insulator film growth. However, a procedure to optimize GaSb oxidation is still an open issue.

Here, a combined scanning-tunneling microscopy (STM) and scanning-tunneling spectroscopy (STS) study of the initial stages of GaSb(100) oxidation is reported. We start with a clean GaSb(100)(4×3) surface,[19] which is then oxidized in different conditions. By combining the unveiled STM/STS features with previous XPS results, we suggest that the density of states above midgap correlates strongly

[a)]Authors to whom correspondence should be addressed. Electronic addresses: jaakko.m.makela@utu.fi; pekka.laukkanen@utu.fi; and rmwallace@utdallas.edu.

with the initial oxygen incorporation. The initial stages for oxygen incorporation, which explain the found increase in a density of states, are suggested. Finally, a method is presented to modify the effects of the GaSb oxidation.

Experiments were carried out in an ultrahigh-vacuum (UHV) multi-chamber system. GaSb(100) substrate pieces were first cleaned by cycles of Ar-ion sputtering (1.0 kV, 4 mA, 5×10^{-8} mbar) and post heating in UHV at 450 °C so that a clear (1×3) low-energy electron diffraction (LEED) appeared (supplementary Fig. S1).[20] STM measurements from this surface revealed a typical dimer-row structure, as shown in Fig. 1,

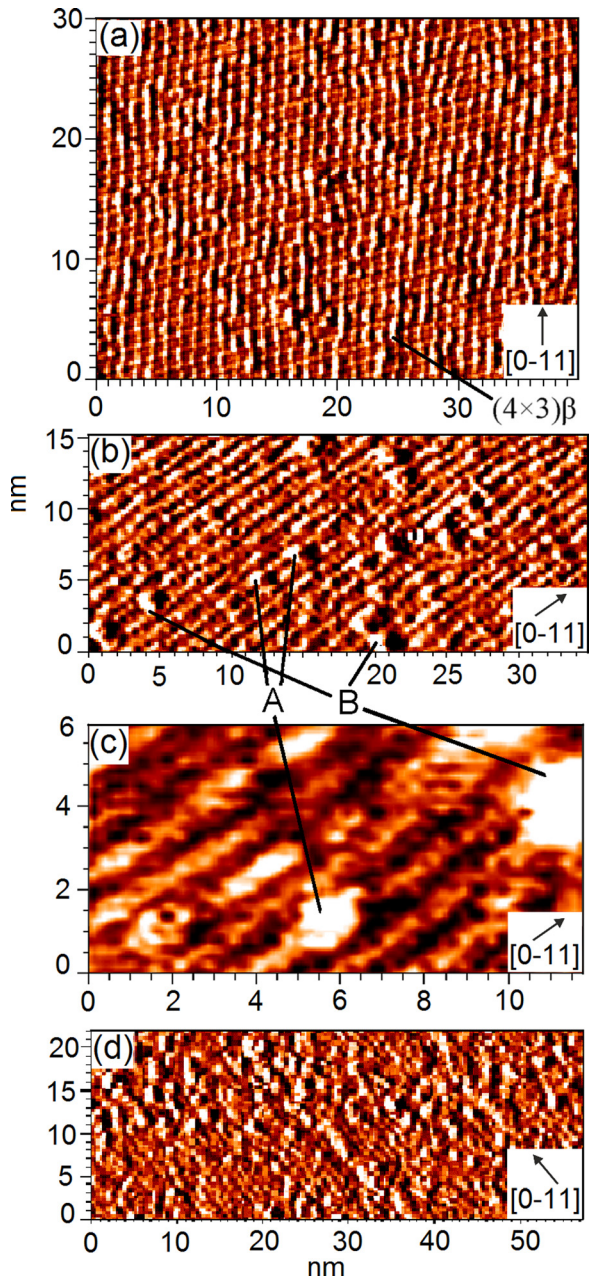

FIG. 1. (a) Filled-state STM image ($V_g = -1.86$ V and $I_t = 0.04$ nA) from clean GaSb(100)(4×3) of which atomic structure can be described with the $(4 \times 3)\alpha$ phase and local $(4 \times 3)\beta$ exemplified (see Fig. 2). (b) Filled-state STM image ($V_g = -3.05$ V and $I_t = 0.26$ nA) from GaSb(100)(4×3) oxidized at 400 °C, 2×10^{-6} mbar O_2, and 10 min (≈1200 L); two types of initial oxidation-induced defects, A and B, are indicated. (c) Filled-state zoomed-in image from the surface described in (b). (d) Filled-state STM image ($V_g = -3.16$ V and $I_t = 0.06$ nA) of GaSb(100)(4×3) oxidized at room temperature, 5×10^{-4} mbar O_2, and 10 min ($\approx 0.3 \times 10^6$ L).

which can be well described with the $(4 \times 3)\alpha$ and (4×3) β-type building blocks that produce the (1×3) LEED pattern.[19,21] These atomic models are presented in Fig. 2. Thus, the clean surface is labeled GaSb(100)(4×3). Different oxidations (described in detail below) were performed by leaking 99.9999% (6N) purity O_2 gas into UHV via a leak valve (with turbo pumping). MBE-grade indium (6N) evaporation was done with a thermal evaporator in which an In-metal piece was wrapped in a Ta envelope which was heated through the application of direct current. STM measurements were performed in the constant-current mode, and STS current-voltage curves were recorded simultaneously with a topographic imaging with Omicron scanning probe microscope. Afterward, the curves were averaged over the chosen surface area and numerically differentiated to get a density of state distribution.

Oxidation of clean GaSb(100)(4×3) at 400 °C with 2×10^{-6} mbar of O_2 (about 1200 L) still provides a clear (1×3) LEED pattern similar to that of the clean surface. XPS (non-monochromatized Mg Kα) from the same surface (not shown) reveals the incorporation of oxygen. The O 1s emission from a similar oxidized surface is shown in Fig. S2 of supplementary material.[20] The STM images from this surface in Figs. 1(b) and 1(c) show the areas with the initial row structure of the clean GaSb(100)(4×3) and also local oxidation-induced defects appearing as white dots in STM. These defects are categorized here into A and B types. The latter is a larger or extended feature and tends to bridge the adjacent dimer rows. The STM results are consistent with the appearance of (1×3) LEED because LEED is not sensitive to local defects due to a short coherence length

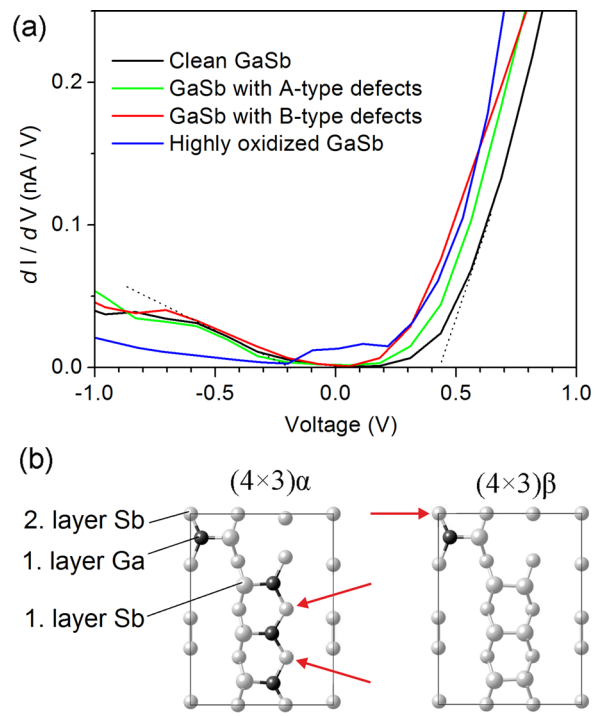

FIG. 2. (a) STS curves measured from GaSb(100)(4×3) oxidized as described in Fig. 1(b) in different areas: clean, type A and type B defective regions. STS curve from the highly oxidized GaSb(100)(4×3), similar to that in Fig. 1(d), is also shown for comparison. (b) The $(4 \times 3)\alpha$ and $(4 \times 3)\beta$ atomic models for GaSb(100)(4×3), and the red arrows indicate the initial atomic sites suggested for the oxygen incorporation.

(5–15 nm) of LEED electrons. When the oxygen exposure was increased to 0.3×10^6 L (at room temperature), which is close to a typical ALD-pulse of an oxygen-containing gas precursor, STM still showed a localized (1×3) dimer-row structure (Fig. 1(d)). However, after this exposure, it is noted that the surface disorder has significantly increased, consistent with a (1×3) LEED pattern which has weakened in intensity and almost disappeared (supplementary Fig. S1).[20] When the 0.3×10^6 L oxidation was done at 200 °C, only weak (1×1) LEED was seen.

The STS-curve analysis for the clean GaSb(100)(4×3) and defective areas is shown in Fig. 2(a). The linear segments of the curve for the bare surface were extrapolated by dotted lines, as depicted in Fig. 2(a). The cutoff of these lines on the voltage axis provides the projections of the valence and conduction band edges of which separation (0.6–0.7 V) is consistent with the GaSb band gap. Figure 2(a) also shows that the density of states increases in the defective areas A and B, in particular, between the Fermi level (0 V) and conduction-band edge (positive voltage side). The curve (Fig. 2(a)) from a disordered area after the high oxidation ($\sim 10^6$ L) shows a further increase in the density of states in the upper part of the band gap and even a metallic feature at the Fermi level.

In Fig. 2(b), the potential atomic sites for the initial oxygen incorporation are presented to be in the second-layer Sb sites of the $(4 \times 3)\alpha$ and $(4 \times 3)\beta$ structures (marked with red arrows). This is based on the following arguments. First, the recent XPS study[9] of oxidation of the well-defined initial GaSb(100)(4×3) surface shows that Ga-O bonds form, but Sb oxidation is not detected. It is indeed reasonable that the amount of Ga-O bonds becomes maximized in the initial oxygen exposure because Ga-O formation is energetically much more favored than Sb-O.[15] Also, the recent investigation of the InSb oxidation indicates that the oxidation starts with substituting subsurface Sb by O.[22,23] This suggests that the first-layer Sb-Sb and Sb-Ga dimers are not disintegrated at the initial stage of oxygen exposure, which can explain the STM and LEED observations that the $\times 3$ dimer-row structure appears on the surface also after a prolonged oxidation. Furthermore, our recent investigation on the oxidation of Sb films[24] shows that higher oxidation temperature (about 500 °C) and longer exposures, compared to that employed here, are needed to promote the Sb oxidation with similar O_2 pressures.

Subsequently, an interesting question arises as to what happens to the extra Sb atoms relieved from the subsurface bonding sites due to the O incorporation. Most likely, the Sb atoms move outwards toward the surface. At the 400 °C substrate temperature (used in Fig. 1(b)), the relieved Sb atoms might also evaporate from the surface. This would explain why the initial (1×3) dimer-row structure is surprisingly stable against the oxidation conditions used. However, it can be expected that at lower temperatures (e.g., 200–300 °C used in ALD), Sb remains on the surface but is not initially oxidized.[9] This implies that metallic Sb can be enriched on the surface due to the oxidation process.

The type B defect (Fig. 1(b)) exhibits an extended feature perpendicular to the dimer rows (i.e., bridging the adjacent rows), which can arise from the relieved Sb atom(s) that is re-bonded rather than evaporated from the surface. Thus, the increased density of empty states above the Fermi level for the features A and B can arise from an increased Sb-Sb bonding, consistent with the previous XPS and C-V results.[14] Another reason is that the Ga dangling-bond state, which initially lies in the conduction band, is lowered toward the gap and valence band due to the formation of Ga-O. It is worth noting that the Sb substitution with O provides one extra valence electron.

The previous[4–10,14] and current findings indicate that the Sb concentration at the GaSb surface (interface) should be minimized to decrease the amount of defect states at insulator/GaSb interfaces. It appears that the problem is not the formation of Sb_2O_3 itself (or other Sb-oxide phase) because the Sb_2O_3 band gap is 3–4 eV.[24] Furthermore, it can be expected that the Van der Waals type bonding between the Sb_4O_6 bicyclic cages can flexibly accommodate the structure with the GaSb lattice. However, such a weakly bonded structure can be also problematic because it is not stable enough, resulting in its decomposition into elemental Sb or suboxides. The minimization of the Sb surface concentration is not straightforward in practice. One reason for this is related to the intrinsic surface structures of GaSb(100), among which the $(4 \times 3)\alpha$ phase is in fact the least Sb-rich structure. Namely, pure GaSb(100) does not have the (4×2) or $c(8 \times 2)$ reconstruction which is the most III group-rich phase for many III-As(100) surfaces.

Therefore, we investigated a method to overcome this problem. We first tested how a monolayer (ML) of indium behaves on the clean GaSb(100)(4×3) surface. After the In deposition at room temperature and the post heating at 400–450 °C in UHV, LEED showed a (4×2) pattern (supplementary Fig. S1).[20] The STM characteristics of this GaSb(100)(4×2)-In reconstruction can be seen in the right top corner of Fig. 3(a). The atomic structure of GaSb(100)(4×2)-In has not yet been thoroughly studied, but preliminarily studies indicated that it can closely resemble the counterpart GaAs(100)(4×2)-In structure.[25] The oxidation of GaSb(100)(4×2)-In with the same parameters as for the clean surface above (Fig. 1(b)) provides again a (1×3) LEED (supplementary Fig. S1),[20] similar to that obtained from the clean surface, coexisting with (4×2) LEED. However, STM images from this oxidized surface reveal the formation of a different (1×3)-ordered phase, which clearly diverges from the clean GaSb(100)(4×3) surface phases. This oxidized phase is labeled (1×3)-In-O, and its structure is presented in the STM image of Fig. 3(a) together with the GaSb(100)(4×2)-In phase. The prolonged oxidation of this surface in the same conditions changes the LEED pattern to a purely (1×3) reconstruction, and the corresponding STM image is shown in Fig. 3(b). XPS confirmed the presence of both In and O. The GaSb(100)(1×3)-In-O surface can be characterized by oxidation-induced white dots of which long-range order is better than that of the oxidation features on GaSb(100)(4×3) without indium. It is interesting that the small amount of In provides the oxidation-induced structure to accommodate the GaSb(100) lattice, consistent with the previous calculations.[26]

Thus, GaSb(100)(1×3)-In-O is a hitherto unreported member for the crystalline oxidized III–V surfaces,[27] which

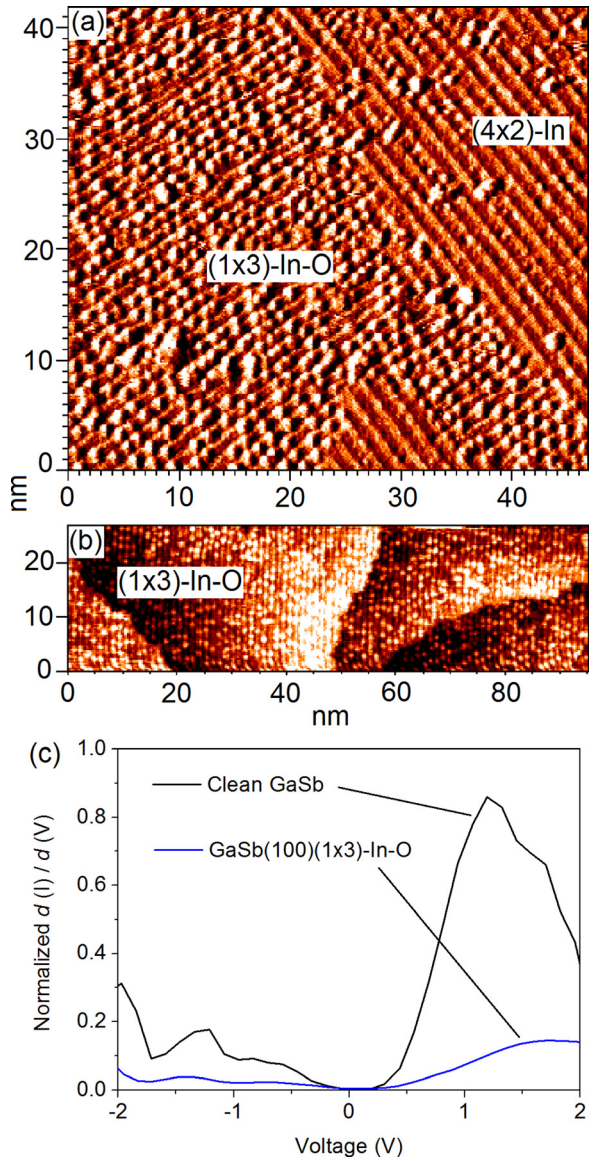

FIG. 3. (a) Filled-state STM image ($V_g = -3.59$ V and $I_t = 0.42$ nA) measured from GaSb(100) after the In-deposition and oxidation at 400 °C, 2×10^{-6} mbar O_2, and 10 min (≈1200 L). The surface includes both the GaSb(100)(4 × 2)-In and GaSb(100)(1 × 3)-In-O areas. (b) Filled-state STM image ($V_g = -3.80$ V and $I_t = 0.04$ nA) measured from pure GaSb(100) (1 × 3)-In-O oxidized at 400 °C, 2×10^{-6} mbar O_2, and 15 min (≈1800 L). (c) Comparison of STS curves between clean GaSb(100)(4 × 3) and oxidized GaSb(100)(1 × 3)-In-O.

have been shown to potentially decrease the defect densities at insulator/III-V interfaces.[28–30] The density of disorder-induced point defects can also be expected to decrease on GaSb(100)(1 × 3)-In-O, but it is still unclear what kind of band structure is formed in the building block(s) of GaSb(100)(1 × 3)-In-O itself, in relation to the GaSb band gap area. To clarify this, a comparison of the STS curves of GaSb(100)(4 × 3) and (1 × 3)-In-O is shown in Fig. 3(c). The comparison suggests that the (1 × 3)-In-O structure does not cause defect states in the GaSb gap.

In conclusion, STM results show that oxidation of the initially well-ordered GaSb(100)(4 × 3) causes disordering (or amorphization) of the surface. Atomic scale STM images together with the STS analysis reveal that the initial stages of oxygen incorporation lead to the formation of unoccupied defect states in the upper part of the gap. When coupled with the previous XPS findings,[9] we suggest that the initial stages of oxidation of GaSb(100)(4 × 3) includes the substitution of second-layer Sb by O and the subsequent Sb enrichment on the surface, which is detrimental to the quality of GaSb-based interfaces. To reduce harmful effects of the GaSb oxidation, we report a method to prepare the GaSb(100)(4 × 2)-In surface and oxidize it into the form of previously unreported phase of crystalline oxidized (1 × 3)-In-O. The presented findings provide an atomic-scale comparison for calculations to advance the understanding of the oxidation process and its effects on the band structure.

[1]A. A. Demkov and A. Navrotsky, *Materials Fundamentals of Gate Dielectrics* (Springer, 2005).
[2]S. Oktyabrsky and P. D. Ye, *Fundamentals of III-V Semiconductor MOSFETs* (Springer, 2010).
[3]L. Lin and J. Robertson, Appl. Phys. Lett. **98**, 082903 (2011).
[4]A. Ali, H. S. Madan, A. P. Kirk, D. A. Zhao, D. A. Mourey, M. K. Hudait, R. M. Wallace, T. N. Jackson, B. R. Bennett, J. B. Boos, and S. Datta, Appl. Phys. Lett. **97**, 143502 (2010).
[5]A. Nainani, Y. Sun, T. Irisawa, Z. Yuan, M. Kobayashi, P. Pianetta, B. R. Bennett, J. Brad Boos, and K. C. Saraswat, J. Appl. Phys. **109**, 114908 (2011).
[6]A. Nainani, T. Irisawa, Z. Yuan, B. Bennett, J. Boos, Y. Nishi, and K. Saraswat, IEEE Trans. Electron Devices **58**, 3407 (2011).
[7]M. Xu, R. Wang, and P. D. Ye, IEEE Electron Device Lett. **32**, 883 (2011).
[8]L. B. Ruppalt, E. R. Cleveland, J. G. Champlain, S. M. Prokes, J. B. Boos, D. Park, and B. R. Bennett, Appl. Phys. Lett. **101**, 231601 (2012).
[9]D. M. Zhernokletov, H. Dong, B. Brennan, J. Kim, R. M. Wallace, M. Yakimov, V. Tokranov, and S. Oktyabrsky, J. Vac. Sci. Technol., A **31**, 060602 (2013).
[10]E. R. Cleveland, L. B. Ruppalt, B. R. Bennett, and S. Prokes, Appl. Surf. Sci. **277**, 167 (2013).
[11]V. Bermudez, J. Appl. Phys. **114**, 024903 (2013).
[12]K. Xiong, W. Wang, D. M. Zhernokletov, K. C. Santhosh, R. C. Longo, R. M. Wallace, and K. Cho, Appl. Phys. Lett. **102**, 022901 (2013).
[13]V. M. Bermudez, Appl. Phys. Lett. **104**, 141605 (2014).
[14]N. Miyata, A. Ohtake, M. Ichikawa, T. Mori, and T. Yasuda, Appl. Phys. Lett. **104**, 232104 (2014).
[15]S. McDonnell, B. Brennan, E. Bursa, R. M. Wallace, K. Winkler, and P. Baumann, J. Vac. Sci. Technol., B **32**, 041201 (2014).
[16]M. Barth, G. B. Rayner, S. McDonnell, R. M. Wallace, B. R. Bennett, R. Engel-Herbert, and S. Datta, Appl. Phys. Lett. **105**, 222103 (2014).
[17]M. Yokoyama, H. Yokoyama, M. Takenaka, and S. Takagi, Appl. Phys. Lett. **106**, 073503 (2015).
[18]D. M. Zhernokletov, H. Dong, B. Brennan, M. Yakimov, V. Tokranov, S. Oktyabrsky, J. Kim, and R. M. Wallace, Appl. Phys. Lett. **102**, 131602 (2013).
[19]W. Barvosa-Carter, A. Bracker, J. Culbertson, B. Nosho, B. Shanabrook, L. Whitman, H. Kim, N. Modine, and E. Kaxiras, Phys. Rev. Lett. **84**, 4649 (2000).
[20]See supplementary material at http://dx.doi.org/10.1063/1.4928544 for LEED and XPS results of the study.
[21]O. Romanyuk, V. M. Kaganer, R. Shayduk, B. P. Tinkham, and W. Braun, Phys. Rev. B **77**, 235322 (2008).
[22]J. J. K. Lång, M. P. J. Punkkinen, M. Tuominen, H.-P. Hedman, M. Vähä-Heikkilä, V. Polojärvi, J. Salmi, V.-M. Korpijärvi, K. Schulte, M. Kuzmin, R. Punkkinen, P. Laukkanen, M. Guina, and K. Kokko, Phys. Rev. B **90**, 045312 (2014).
[23]M. Tuominen, J. Lång, J. Dahl, M. Kuzmin, M. Yasir, J. Mäkelä, J. R. Osiecki, K. Schulte, M. P. J. Punkkinen, P. Laukkanen, and K. Kokko, Appl. Phys. Lett. **106**, 011606 (2015).
[24]M. Yasir, M. Kuzmin, M. P. J. Punkkinen, J. Mäkelä, M. Tuominen, J. Dahl, P. Laukkanen, and K. Kokko, Appl. Surf. Sci. **349**, 259 (2015).
[25]J. J. K. Lång, M. P. J. Punkkinen, P. Laukkanen, M. Kuzmin, V. Tuominen, M. Pessa, M. Guina, I. J. Väyrynen, K. Kokko, B. Johansson, and L. Vitos, Phys. Rev. B **81**, 245305 (2010).

[26]M. Scarrozza, G. Pourtois, M. Houssa, M. Caymax, A. Stesmans, M. Meuris, and M. M. Heyns, Microelectron. Eng. **86**, 1747 (2009).
[27]M. P. J. Punkkinen, P. Laukkanen, J. Lång, M. Kuzmin, M. Tuominen, V. Tuominen, J. Dahl, M. Pessa, M. Guina, K. Kokko, J. Sadowski, B. Johansson, I. J. Väyrynen, and L. Vitos, Phys. Rev. B **83**, 195329 (2011).
[28]C. H. Wang, S. W. Wang, G. Doornbos, G. Astromskas, K. Bhuwalka, R. Contreras-Guerrero, M. Edirisooriya, J. S. Rojas-Ramirez, G. Vellianitis, R. Oxland, M. C. Holland, C. H. Hsieh, P. Ramvall, E. Lind, W. C. Hsu, L.-E. Wernersson, R. Droopad, M. Passlack, and C. H. Diaz, Appl. Phys. Lett. **103**, 143510 (2013).
[29]M. Passlack, S.-W. Wang, G. Doornbos, C.-H. Wang, R. Contreras-Guerrero, M. Edirisooriya, J. Rojas-Ramirez, C.-H. Hsieh, R. Droopad, and C. H. Diaz, Appl. Phys. Lett. **104**, 223501 (2014).
[30]M. Tuominen, M. Yasir, J. Lång, J. Dahl, M. Kuzmin, J. Mäkelä, M. Punkkinen, P. Laukkanen, K. Kokko, K. Schulte, R. Punkkinen, V.-M. Korpijärvi, V. Polojärvi, and M. Guina, Phys. Chem. Chem. Phys. **17**, 7060 (2015).

Oxidation of GaSb(100) and its Control Studied by Scanning Tunneling Microscopy and Spectroscopy

Citation:

Makela, J., M. Tuominen, M. Yasir, M. Kuzmin, et al. 2015. "Oxidation of GaSb(100) and its control studied by scanning tunneling microscopy and spectroscopy." Applied Physics Letters 107(6), doi:10.1063/1.4928544